Recursive Online Compensation of Piezoelectric Nonlinearities via a Modified Prandtl-Ishlinskii Approach

Christopher Schindlbeck * **Christian Pape** *
Eduard Reithmeier *

* *Institute of Measurement and Automatic Control, Faculty of Mechanical Engineering, Leibniz University Hannover, Hanover, Germany (e-mail: christopher.schindlbeck@imr.uni-hannover.de)*

Abstract: Piezoelectric actuators are often employed in micro- and nanopositioning devices due to their extremely fine positioning resolution but exhibit strong nonlinear effects (predominantly hysteresis and creep) which pose a considerable challenge for the control community. For online compensation of these effects, the modified Prandtl-Ishlinskii model is particularly suitable since its inverse can be found analytically by a parameter transformation. However, this model-based approach has not yet made its way to devices that target positioning tasks. Therein, trajectories typically contain segments with varying final times, small ranges of motion, or stationary states such that the hysteresis and creep effects are not optimally excited and frequency-dependence is induced which ultimately leads to a deteriorated compensation performance. This paper proposes an online approach to overcome the problem by taking into account prior hysteresis/creep information in a recursive manner based on databases for better tracking performance and a more robust compensation of the aforementioned nonlinearities. In order to show the efficacy of the proposed approach, experimental results are provided by using trajectories with varying final times, stationary states and alternating small/large ranges of motion on a micro-positioning unit driven by piezoelectric actuators.

Keywords: Hysteresis, Compensation, Actuators, Microsystems, Nonlinear systems

1. INTRODUCTION

In the field of micro- and nanorobotics, a variety of physical actuation principles can be utilized to achieve displacement on small scales. Most actuators in this field rely on electrostatic, electromagnetic, electrothermal or piezoelectric principles, see Nelson et al. (2008).
Piezoelectric actuators are a popular choice due to their (sub)nanometer level resolution, highly dynamic behavior, large blocking force, high mechanical stiffness, and compact size (Xu and Tan (2015)) and have been employed in diverse applications from machining such as milling (Gozen and Ozdoganlar (2012)) or grinding (Tian et al. (2011)) to scanning probe microscopy (Clayton et al. (2009)). However, the downside of piezoelectric actuators are strong hysteresis and creep effects that arise due to inherent material characteristics of the piezoelectric crystals. Model-based control approaches are able to tackle these problems by feedforward compensation through an inverse model. For this, hysteresis and creep effects need to be modeled explicitly first.
Creep can be either modeled linearly e.g. by a series interconnection of mass-spring-damper systems, see Croft et al. (2001) or in a nonlinear form through the application of logarithmic terms, see Jung and Gweon (2000). Hysteresis models are typically classified into physics-based and phenomenological models, see Gu et al. (2016). Physics-based models attempt to relate the observed hysteresis effects to concrete physical parameter and establish a dynamic model thereafter. The most prominent example for this class is the Jiles-Atherton model, see Rosenbaum et al. (2010). Phenomenological models are independent from the physical model and can be further subdivided into differential-based models, operator-based hysteresis models and other hysteresis models such as ellipse-based models (Gu and Zhu (2011)) or neuronal networks (Zhao and Tan (2008)). While differential-based models aim to model hysteresis behavior explicitly via differential equations (Visintin (2013)), operator-based hysteresis models establish a model by superposition of individual elementary operators. For this, these operators are first weighted and then superposed in order to yield the desired overall hysteresis model. The Preisach model (Natale et al. (2001)) employs relay operators as elementary operators (see Mayergoyz (2003)) and the Krasnosel'skii-Pokrovskii model (Galinaitis (1999)) is a straightforward extension of this model utilizing generalized relay operators.
For the control of a piezoelectric actuator, not only mitigation of nonlinear effects is desired but also capabilities that allow for online compensation of said effects, essentially linearizing the actuator at run-time. Here is where the shortcomings of the aforementioned hysteresis models become evident since analytical solutions for the respective inverse models are computationally too expensive for online and real-time applications and therefore have to resort to numerical inverse solutions, see e.g. Song et al. (2005).

The Prandtl-Ishlinskii model can be a remedy due to having an analytical inverse and furthermore its modified version can even cope with asymmetries in the hysteresis. However, trajectories considered in existing literature following this approach are specially designed to excite hysteresis and creep simultaneously and resulting models are tested against these. Furthermore, cycle times for compensation and periodicity of the trajectories coincide.
For real-life applications, such as e.g. pick-and-place trajectories in assembly processes, this is not useful since the trajectories may only excite one nonlinear effect and even only to a small extent. In this paper, we provide a more robust approach for online compensation of nonlinear piezoelectric effects that takes into account prior information in a recursive way so that (at least some portion of) information about the nonlinear effects is conserved. Although recursive identification has already been covered for other models, such as the Preisach model (Tan and Baras (2004)) or the Krasnosel'skii-Pokrovskii model (Webb et al. (1998)), the novelty in the presented approach lies in the recursive usage of databases.
The remainder of this paper is organized as follows. Sec. 2 outlines the hysteresis and creep model via the modified Prandtl-Ishlinskii model and in Sec. 3 its analytical inverse is presented. Sec. 4 covers the novel recursive online compensation algorithm via the modified Prandtl-Ishlinskii model. In Sec. 5 the theory is applied to a micropositioning unit with a pick-and-place-like trajectory. Finally, a conclusion is given in Sec. 6.

2. HYSTERESIS AND CREEP MODELING

First, the mathematical model based on operators for hysteresis and creep effects used in this paper is presented. In the following sections, $x(t)$ denotes the input signal of the operators while $y(t)$ denotes their output signal. For implementation purposes, a time-discrete representation is preferred such that $x(t) = x(k)$ with timestep $k \in \mathbb{N}_0^+$ and $kT_s \leq t < (k+1)T_s$ with sample time T_s. The sections 2 and 3 essentially follow Kuhnen (2008) and Pesotski (2011).

2.1 Play Operator

The discrete elementary play operator is defined as

$$\begin{aligned} y(k) &= H_{r_H}[x(k), y(k-1)] \\ &= \max\{x(k) - r_H, \min\{x(k) + r_H, y(k-1)\}\} \end{aligned} \quad (1)$$

with threshold r_H parameterizing the width of the play operator and corresponding initial condition

$$\begin{aligned} y(0) &= H_{r_H}[x(0), y_{H0}] \\ &= \max\{x(0) - r_H, \min\{x(0) + r_H, y_{H0}\}\}, \end{aligned}$$

where y_{H0} is the initial state of the operator output. In order to model more complex hysteresis behavior, the dot product of a vector of n+1 elementary play operators (from (1) for n+1 different thresholds) and weight vector $\mathbf{w}_H \in \mathbb{R}^{n+1}$ can be used. This leads to the discretized version of the Prandtl-Ishlinskii-Hysteresis operator defined as

$$\begin{aligned} H_\delta[x(k), \mathbf{y}_{H0}] &= \sum_{i=0}^{n} w_{Hi} H_{r_{Hi}}[x(k), y_{H0i}] \\ &= \mathbf{w}_H^T \mathbf{H}_{\mathbf{r}_H}[x(k), \mathbf{y}_{H0}] \end{aligned} \quad (2)$$

with threshold vector $\mathbf{r}_H \in \mathbb{R}^{n+1}$ for n+1 elementary play operators.

2.2 Superposition Operator

The Prandtl-Ishlinskii-Hysteresis operator would suffice for symmetric hysteresis effects. However, in reality, most actuators are characterized by slight asymmetries in the hysteresis which the superposition operator addresses. The discrete elementary superposition operator is defined as

$$S_{r_S}[x(k)] = \begin{cases} \max\{x(k) - r_S, 0\} & \text{for } r_S > 0 \\ \min\{x(k) - r_S, 0\} & \text{for } r_S < 0 \\ 0 & \text{for } r_S = 0 \end{cases}$$

with respective threshold r_S. Again, with a set of weights $\mathbf{w}_S \in \mathbb{R}^{2l+1}$ and thresholds $\mathbf{r}_H \in \mathbb{R}^{2l+1}$ this can be generalized to the so-called discrete Prandtl-Ishlinskii-Superposition operator

$$S_\delta[x(k)] = \sum_{i=-l}^{l} w_{Si} S_{r_{Si}}[x(k)] = \mathbf{w}_S^T \mathbf{S}_{\mathbf{r}_S}[x(k)], \quad (3)$$

where $2l$+1 denotes the number of elementary superposition operators used for the model.

2.3 Creep Operator

In order to fit the aforementioned operator paradigm for creep effects, Kuhnen (2005) presented a seamless integration by an operator-based creep representation. The discrete elementary creep operator is given as

$$K_{r_K}[x(k), \mathbf{y}_{K0}(r_K)] = \frac{1}{m} \sum_{j=1}^{m} K_{r_K a_K}[x(k), y_{K0}(r_K, a_{Kj})]$$

with threshold r_K and m (sub-)elementary creep operators $K_{r_K a_K}$ with respective creep eigenvalues

$$a_{Kj} = \frac{1}{10^{j-1} T_s} \text{ for } j = 1, ..., m$$

such that $a_{K1} > a_{K2} > ... a_{Km} > 0$ holds. $K_{r_K a_K}$ can be obtained analytically from a differential equation yielding the solution

$$y(k) = y(k-1) + (1 - e^{-a_K T_s}) H_{r_K}[x(k-1) - y(k-1), 0],$$

where

$$y(k) = K_{r_K a_K}[x(k-1), y(k-1), a_K].$$

Next, the discrete Prandtl-Ishlinskii-Creep operator can be defined (in analogy to (2) and (3)) as

$$\begin{aligned} K_\delta[x(k), \mathbf{Y}_{K0}] &= \sum_{i=0}^{n} w_{Ki} K_{r_{Ki}}[x(k), \mathbf{y}_{K0i}] \\ &= \mathbf{w}_K^T \mathbf{K}_{\mathbf{r}_K}[x(k), \mathbf{Y}_{K0}]. \end{aligned} \quad (4)$$

2.4 Combined Model

Now, a unified model for hysteresis and creep effects can be established by combining the operators from (2), (3), and (4) as

$$\begin{aligned} \Gamma[x(k), \mathbf{y}_{H0}, \mathbf{Y}_{K0}] &= S_\delta[H_\delta[x(k), \mathbf{y_{H0}}] + K_\delta[x(k), \mathbf{Y}_{K0}]] \\ &= \mathbf{w}_S^T \mathbf{S}_{\mathbf{r}_S} (\mathbf{w}_H^T \mathbf{H}_{\mathbf{r}_H}[x(k), \mathbf{y}_{H0}] \\ &\quad + \mathbf{w}_K^T \mathbf{K}_{\mathbf{r}_K}[x(k), \mathbf{Y}_{K0}]) \\ &= \mathbf{w}_S^T \mathbf{S}_{\mathbf{r}_S} \left(\mathbf{w}_{HK}^T \mathbf{H}_{HK}[x(k), \mathbf{y}_{H0}, \mathbf{Y}_{K0}]\right) \end{aligned} \quad (5)$$

with $\mathbf{w}_{HK}^T := \left(\mathbf{w}_H^T, \mathbf{w}_K^T\right)$ and

$$\mathbf{H}_{HK}[x(k), \mathbf{y}_{H0}, \mathbf{Y}_{K0}]) := \begin{pmatrix} \mathbf{H}_{\mathbf{r}_H}[x(k), \mathbf{y}_{H0}] \\ \mathbf{K}_{\mathbf{r}_K}[x(k), \mathbf{Y}_{K0}] \end{pmatrix}.$$

Γ from (5) is known as the modified Prandtl-Ishlinskii operator.

3. INVERSE MODEL

As already mentioned in Sec. 1, the (modified) Prandtl-Ishlinskii model allows for an analytical inverse since the model is identical except for its weights and thresholds. For the inverse operators, the weights, thresholds, and initial conditions can be derived by an algebraic parameter transformation. This will be outlined in more detailed in the following.

3.1 Inverse Play Operator

The inverse play operator is defined as

$$H_\delta^{-1}[y(k), \mathbf{z}'_{H0}] = \mathbf{w}_H'^T \mathbf{H}_{\mathbf{r}'_H}[y(k), \mathbf{z}'_{H0}]$$

with corresponding weights

$$w'_{H0} = w_{H0}^{-1}$$
$$w'_{Hi} = \frac{w_{Hi}}{\left(\sum_{j=0}^{i} w_{Hj}\right)\left(\sum_{j=0}^{i-1} w_{Hj}\right)} \text{ for } i = 1, ..., n$$

and thresholds

$$r'_{Hi} = \sum_{j=0}^{i} w_{Hj}(r_{Hi} - r_{Hj}) \text{ for } \; i = 0, ..., n.$$

For the inverse play operator the corresponding initial conditions $\mathbf{z}'_{H0}$ are needed which are defined as

$$z'_{H0i} = \sum_{j=0}^{i} w_{Hj} z_{H0i} + \sum_{j=i+1}^{n} w_{Hj} z_{H0j}, \text{ for } i = 0, ..., n.$$

3.2 Inverse Superposition Operator

Similarly, the inverse superposition operator

$$S_\delta^{-1}[y(k)] = \mathbf{w}_S'^T \mathbf{S}_{\mathbf{r}'_S}[y(k)]$$

takes the form of (3) with corresponding weights defined as

$$w'_{Si} = \frac{w_{Si}}{\left(w_{S0} + \sum_{j=i}^{-1} w_{Sj}\right)\left(w_{S0} + \sum_{j=i+1}^{-1} w_{Sj}\right)}$$

for $i = -l, ..., -1$, $w'_{S0} = \frac{1}{w_{S0}}$, and

$$w'_{Si} = \frac{w_{Si}}{\left(w_{S0} + \sum_{j=1}^{i} w_{Sj}\right)\left(w_{S0} + \sum_{j=1}^{i-1} w_{Sj}\right)}$$

for $i = 1, ..., l$. The respective thresholds are

$$r'_{Si} = \sum_{j=i}^{0} w_{Sj}(r_{Si} - r_{Sj}) \text{ for } i = -l, ..., -1 \text{ and}$$

$$r'_{Si} = \sum_{j=0}^{i} w_{Sj}(r_{Si} - r_{Sj}) \text{ for } i = 1, ..., l$$

with $r'_{S0} = 0$.

3.3 Inverse Combined Model

Now, it is possible to combine the inverse operators to obtain a combined inverse modified Prandtl-Ishlinskii operator $\Gamma^{-1}[y(k), \mathbf{y}'_{H0}, \mathbf{Y}'_{K0}]$ as

$$\begin{aligned} x(k) &= \Gamma^{-1}[y(k), \mathbf{y}'_{H0}, \mathbf{Y}'_{K0}] \\ &= H_\delta^{-1}\left[S_\delta^{-1}[y(k)] - K_\delta[x(k), \mathbf{Y}_{K0}], \mathbf{y}'_{H0}\right]. \end{aligned} \quad (6)$$

It should be noted that this shows that there is no necessity to invert the creep operator.

4. RECURSIVE ONLINE COMPENSATION

In this section, a novel cost function is introduced taking recursive information into account from which a quadratic optimization problem can be derived. Solving this problem yields the weights for online compensation of piezoelectric nonlinearities. Fig. 1 depicts the block diagram for the compensation structure.

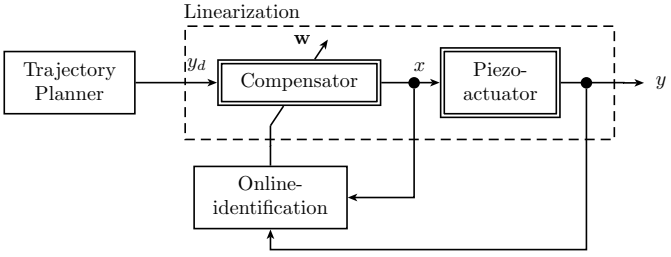

Fig. 1. Block diagram of feedforward compensation structure with weight adaption. Desired values y_d are generated by a trajectory planner.

4.1 Cost Function with Recursive Information

The continuous cost function with recursive information is defined as

$$V(t_f) = \sum_{i=0}^{N_t - 1} \int_{t_{f-i-1}}^{t_{f-i}} E^2(t)\, dt \quad (7)$$

with initial time $t_0 = t_{f-N_t}$ and final time t_f such that the interval is partitioned in $N_t \geq 1$ databases as $[t_0, t_1, ..., t_f] \in \mathbb{R}^{N_t+1}$ which are considered for optimization. Here, each database has a fixed length consisting of N_k data points [1]. The error E is composed of the difference between model output of (5) and actuator output as follows

$$E(k) = H_\delta[x(k)] + K_\delta[x(k)] - S_\delta^{-1}[y(k)]$$

and can be rearranged into linear form

$$E(k) = x(k) + \mathbf{w}^T \mathbf{\Phi}[x(k), y(k)] \quad (8)$$

with

$$\mathbf{w} = \begin{pmatrix} \tilde{\mathbf{w}}_H \\ \mathbf{w}'_S \\ \mathbf{w}_K \end{pmatrix}, \; \mathbf{\Phi}[x(k), y(k)] = \begin{pmatrix} \tilde{\mathbf{H}}_{\mathbf{r}_H}[x(k)] \\ -\mathbf{S}_{\mathbf{r}'_S}[y(k)] \\ \mathbf{K}_{\mathbf{r}_K}[x(k)] \end{pmatrix},$$

and

$$\mathbf{w}_H = \begin{pmatrix} 1 \\ \tilde{\mathbf{w}}_H \end{pmatrix}, \; \tilde{\mathbf{H}}_{\mathbf{r}_H} = \begin{pmatrix} H_{r_{H1}}[x(k)] \\ \vdots \\ H_{r_{Hn}}[x(k)] \end{pmatrix}.$$

[1] Of course databases with different lengths could be considered, but this is straightforward and would only make the notation cumbersome.

The squared error E^2 obtained from (8) is

$$E^2(k) = \mathbf{w}^T \mathbf{\Phi}(k)\mathbf{\Phi}^T(k)\mathbf{w} + 2x(k)\mathbf{\Phi}^T(k)\mathbf{w} + x^2(k),$$

such that the discretized version of the recursive cost function (7) reads

$$\begin{aligned} V &= \frac{1}{2}\sum_{i=0}^{N_t-1}\sum_{k=iN_k}^{(i+1)N_k} E^2(k) \\ &= \sum_{i=0}^{N_t-1}\Bigg\{\frac{1}{2}\mathbf{w}^T \underbrace{\sum_{k=iN_k}^{(i+1)N_k}\mathbf{\Phi}(k)\mathbf{\Phi}^T(k)}_{=:\mathbf{A}_i}\mathbf{w} + \\ &\qquad \underbrace{\sum_{k=iN_k}^{(i+1)N_k} x(k)\mathbf{\Phi}^T(k)}_{=:\mathbf{b}_i^T}\mathbf{w} + \frac{1}{2}\underbrace{\sum_{k=iN_k}^{(i+1)N_k} x^2(k)}_{=:\mathbf{c}_i}\Bigg\} \\ &= \sum_{i=0}^{N_t-1}\left\{\frac{1}{2}\mathbf{w}^T\mathbf{A}_i\mathbf{w} + \mathbf{b}_i^T\mathbf{w} + \frac{1}{2}\mathbf{c}_i\right\} \\ &= \frac{1}{2}\mathbf{w}^T\underbrace{\sum_{i=0}^{N_t-1}\mathbf{A}_i}_{=:\mathbf{A}_{i+1}}\mathbf{w} + \underbrace{\sum_{i=0}^{N_t-1}\mathbf{b}_i^T}_{=:\mathbf{b}_{i+1}^T}\mathbf{w} + \frac{1}{2}\underbrace{\sum_{i=0}^{N_t-1}\mathbf{c}_i}_{=:\mathbf{c}_{i+1}}. \end{aligned} \tag{9}$$

4.2 Optimization Problem

From (9), the recursive rule

$$\mathbf{A}_{i+1} = \sum_{i=0}^{N_t-1}\mathbf{A}_i,\ \mathbf{b}_{i+1} = \sum_{i=0}^{N_t-1}\mathbf{b}_i$$

is derived for the quadratic optimization problem

$$\min_{\mathbf{w}} \frac{1}{2}\mathbf{w}^T\mathbf{A}_{i+1}\mathbf{w} + \mathbf{b}_{i+1}^T\mathbf{w}$$

with corresponding linear inequality constraints [2]. This is an extension to existing algorithms in literature which only consider $N_t = 1$ (i.e. one database).

5. EXPERIMENTAL VERIFICATION

Next, experimental verification of the recursive online compensation is provided.

5.1 Description of Experimental Setup

The piezoelectric micro-positioning unit *XYZ200M* from *Cedrat Technologies* with 3 degrees of freedom is used for experimental verification, see Fig. 2a. The X- and Y-axes follow antagonistic design, i.e. two opposing piezoelectric actuators for each of axis, respectively (see Fig. 2b). This enhances point-symmetry of the hysteresis curve. The Z-axis is actuated by three piezoelectric actuators placed in circular manner. Therefore, there are seven piezoelectric actuators in total, where each actuator consists of two stacks of piezoelectric ceramics in order to amplify displacement. Each actuator is furthermore preloaded by an external spring shell made of stainless steel also protecting e.g. against tensile stress, see Fig. 2c. The unit weighs about 540 g with a nominal displacement of 200 μm (nanoscopic resolution of 2 nm) and a nominal blocked force of 118 N in each Cartesian direction.

[2] For sake of brevity, the interested reader is referred to Kuhnen (2008) for a detailed derivation of the inequality constraints.

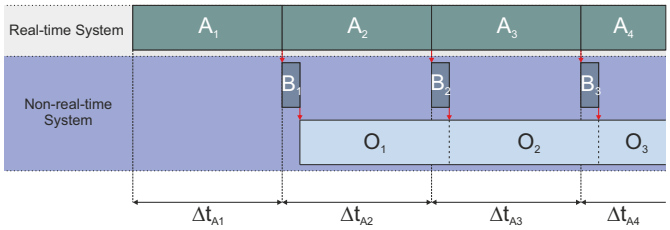

Fig. 3. Schematic depiction of data acquisition phase (A), building of (recursive) database (B), and optimization phase (O) on real-time system and non-real-time system.

A *National Instruments PXI* real-time system is used to command voltage input and access strain-gauge measurements via a digital I/O interface with 1 kHz sampling frequency. The commanded voltage is furthermore amplified by a voltage amplifier by a factor of 20 and is then equally applied across each piezoelectric ceramic stack (i.e. four for the X- and Y-axes, six for the Z-axis), only one stack per axis is equipped with a strain gauge sensor, respectively. Measurement data is acquired on the real-time system (A) while building the (recursive) database (B) as well as optimization of the recursive cost function (O) takes place on a non-real-time system, see Fig. 3. The reasons for this division of labor is that the optimization leads to computationally intensive calculations that would violate real-time constraints on the real-time system. The weights from the optimization procedure are continuously transfered to the real-time system for compensation purposes.

5.2 Choice of Trajectory

For the subsequent experiments, trajectories comprised of quintic polynomials and stationary states in an alternating manner are used. Such trajectories are typically employed in pick-and-place tasks where a smooth transition between two points is desired and sufficient time for gripping/releasing an object is necessary meaning the tool center point must be at rest for a certain amount of time. Such stationary states are especially problematic for the identification of hysteresis effects and hence for their compensation since they do not excite the actuator over a certain (larger) range of motion. In contrast, creep effects are minimally excited when a smooth trajectory without stationary states is executed. Furthermore, final time of the polynomials is varied which alters the frequency of the input signal.
The following results are shown for the X-axis of the micro-positioning unit without loss of generality and the theory can be applied to the other axes in a straightforward fashion.

5.3 Results for Final States $y_{d,f} \in \{-3, 0, 3\}\,[V]$

In Fig. 4 a trajectory of the aforementioned type is commanded as desired trajectory. Therein, $N_k = 1000$ (i.e. a database length of one second) is chosen. For the case of one database, $N_t = 1$ (blue), there is not sufficient

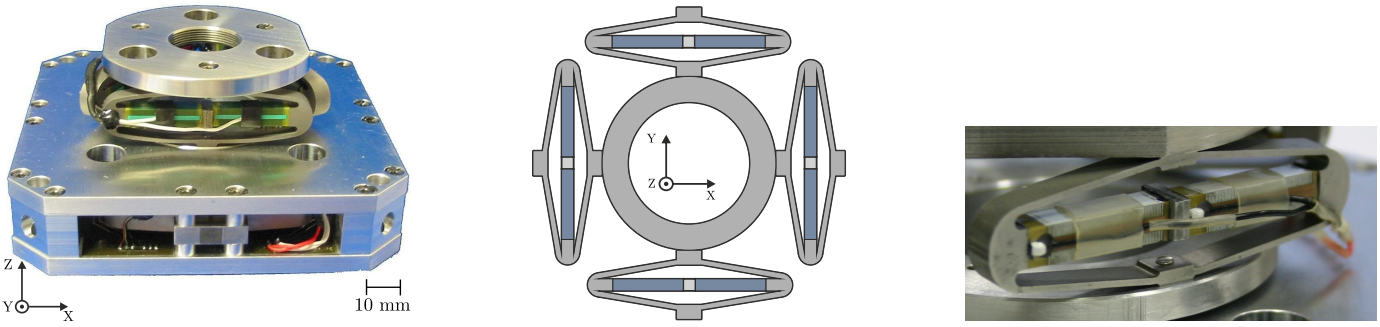

(a) Piezoelectric micro-positioning unit (b) Schematic cross-section (c) Single piezoelectric actuator of Z-axis

Fig. 2. Piezoelectric micro-positioning unit with 3 degrees of freedom (a), schematic cross-section of X-Y-plane (b), and close up view of a single actuator (c).

time for the convergence of weights which results in undesired oscillation (at $t \approx 5.6\,\mathrm{s}$) and therefore in an error that furthermore propagates forward for each upcoming optimization step. This induces a phase delay which does not recover over time.

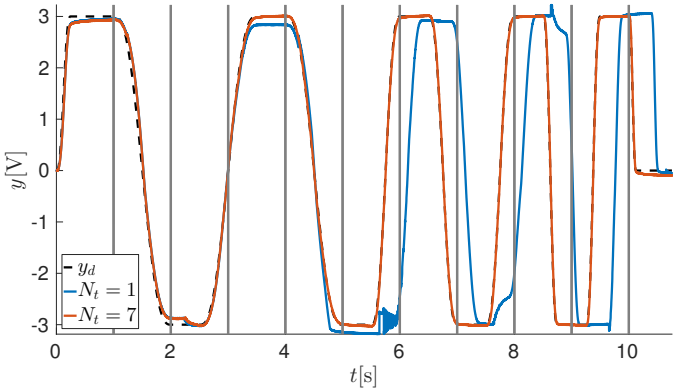

Fig. 4. Results for a pick-and-place-like trajectory with $N_k = 1000$ for $N_t = 1$ (blue) and $N_t = 7$ (red). Vertical gray lines indicate the beginning of a new database.

For multiple databases, $N_t = 7$, the result is a stable compensator yielding satisfactory tracking performance.
In Fig. 5 (top) the database length is increased to $N_k = 4000$ for the same trajectory. Here, both $N_t = 1$ and $N_t = 7$ lead to a stable tracking performance with good compensation results. However, a closer look at the tracking error (see Fig. 5 (middle)) reveals higher deviations from the desired trajectory for $N_t = 1$ than for $N_t = 7$. This is exemplified in close up views, see Fig. 5a-5f. Not only does the recursive approach provide better tracking results (see Fig. 5a and Fig. 5d-5f) but it is also less sensitive to a newly incoming database (Fig. 5b-5c). Evaluating the normalized root mean square error (NRMSE)

$$\mathrm{NRMSE}(y_d, y) = \frac{\|y_d - y\|_2}{\|y_d\|_2} \tag{10}$$

yields 0.0340 for $N_t = 1$ and 0.0336 for $N_t = 7$, i.e. an increase of 1.33 % in tracking performance.

5.4 Results for Final States $y_{d,f} \in \{-3, -1, 0, 1, 3\}\,[V]$

In Fig. 6, certain segments of the trajectory do not traverse the full range of motion of the piezoactuator and therefore hysteresis characteristics are not optimally excited. This is especially problematic when a small database is chosen, see here $N_k = 1000$ without taking into account prior information. At $t = 11\,\mathrm{s}$ when the full range of motion is traversed for the first time after passages with a lower range of motion, the subsequent compensation is not satisfactory and results in a large tracking error. In contrast, when choosing the recursive approach with consideration of prior information, good compensation results can be observed. Furthermore, a small database can lead to oscillating behavior (c.f. $t \in [18, 19]$ and $t \in [20, 21]$) which may destabilize the system as already seen in Fig. 4. The compensation does not suffer from the aforementioned problems by choosing a larger database (here $N_k = 4000$). However, due to the acquisition phase being longer, there is no compensation at the beginning of the trajectory (c.f. $t \in [0, 4]$) as compared to a small database with recursive approach. Here, the NMRSE without recursive online approach is 0.0736 for $N_k = 1000$ and 0.0675 for $N_k = 4000$, and for the recursive online approach 0.0397, i.e. the recursive approach results in an 46.02 % improvement as compared to the approach with one database of length $N_k = 1000$ and 41.16 % as compared to $N_k = 4000$ using the NRMSE.

6. CONCLUSION

In this paper, a recursive online compensation via the modified Prandtl-Ishlinskii model has been proposed. By taking into account prior information in the construction of a database, changes in the nonlinear effects are handled more robustly. This becomes evident when a newly incoming database contains different information in the hysteresis/creep composition than the prior one. Furthermore, the overall tracking performance has increased by taking into account multiple smaller databases. Although in principle this could also be achieved by taking large databases, this decreases reaction time and databases over longer time periods may contain greater changes in between two databases which would lead to larger changes in the weights and potentially destabilize tracking due to oscillating weight convergence.

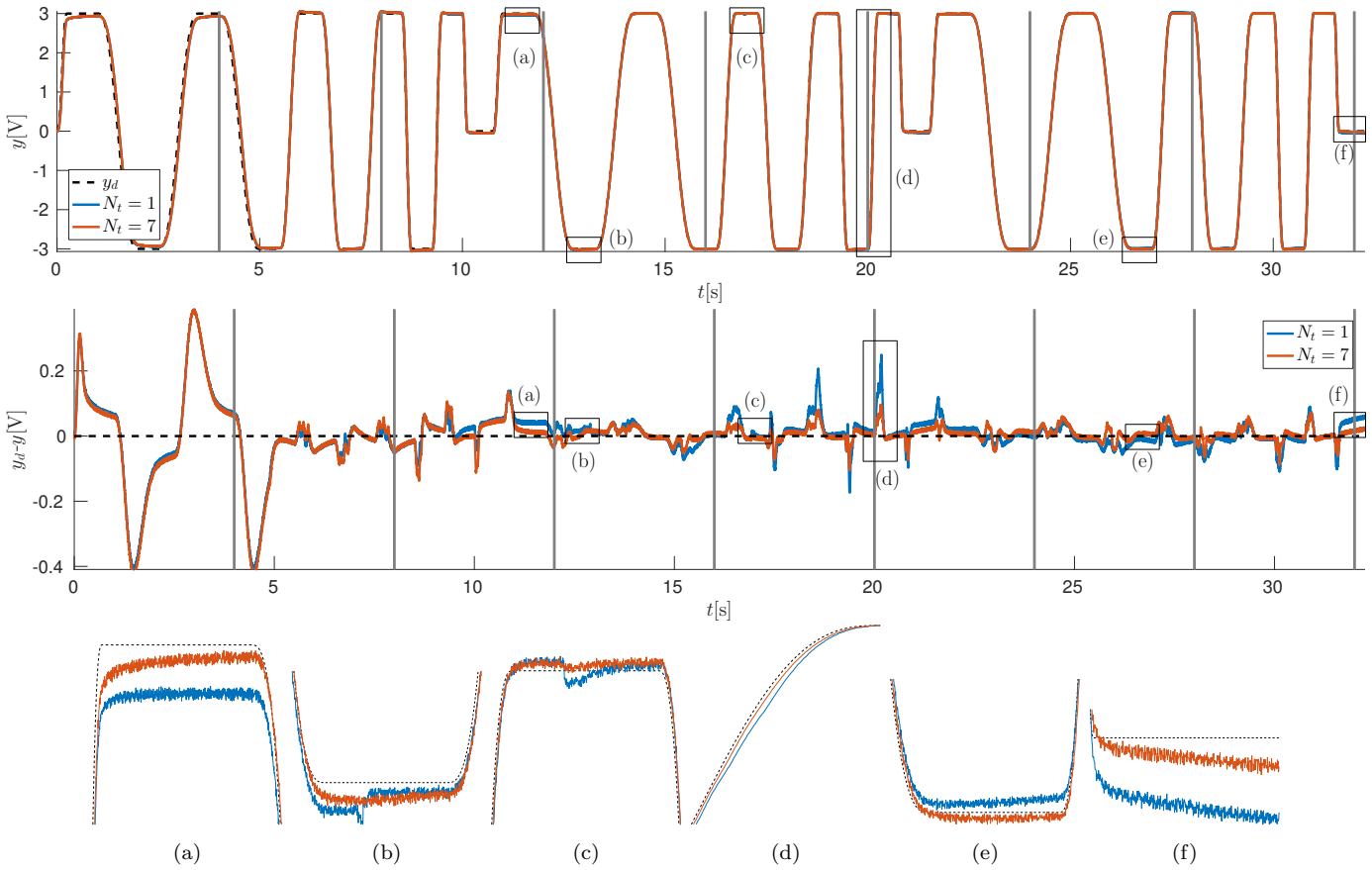

Fig. 5. Experimental results for trajectories with final states $y_{d,f} \in \{-3, 0, 3\}$. Tracking (top) and tracking error (middle) with close up views (5a-5f) for $N_t = 1$ (red) and $N_t = 7$ (blue).

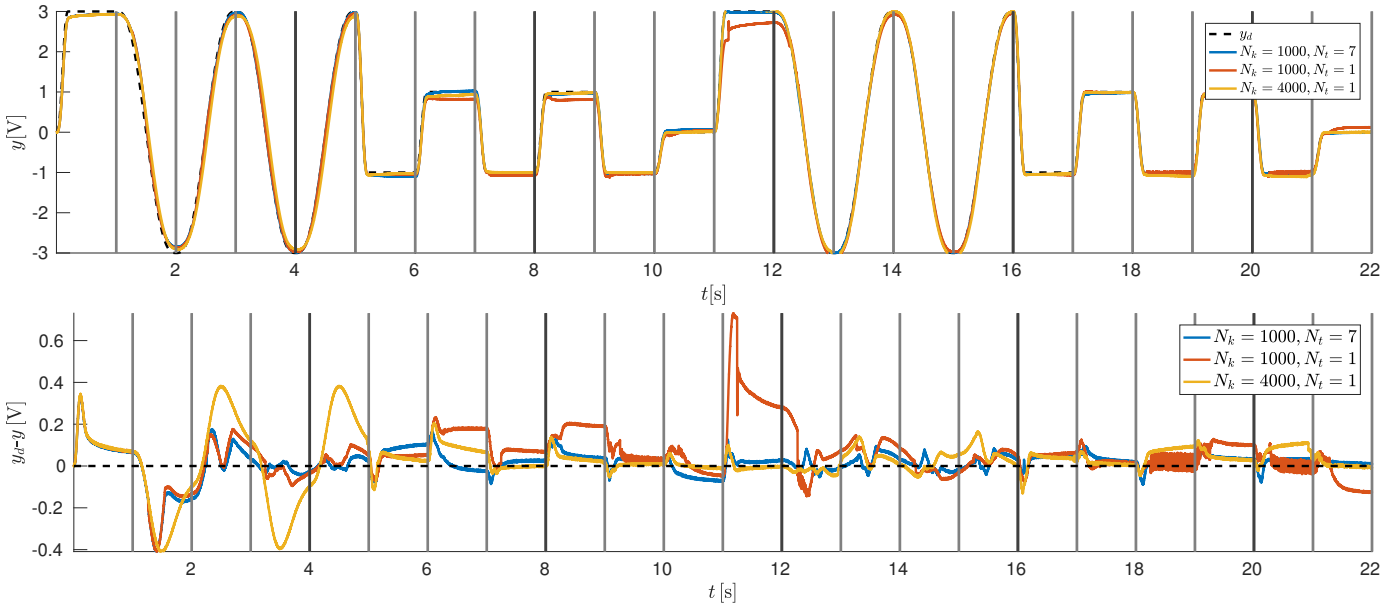

Fig. 6. Experimental results for trajectories with final states $y_{d,f} \in \{-3, -1, 0, 1, 3\}$. Tracking (top) and tracking error (bottom) for $N_k = 1000, N_t = 7$ (blue) and $N_k = 1000, N_t = 1$ (red) and $N_k = 4000, N_t = 1$ (yellow). Vertical gray lines indicate the beginning of a new database for $N_k = 1000$ and vertical black lines for $N_k = 4000$.

ACKNOWLEDGEMENTS

We would like to thank Nils Melchert for his valuable contribution to this work.

REFERENCES

Clayton, G.M., Tien, S., Leang, K.K., Zou, Q., and Devasia, S. (2009). A review of feedforward control approaches in nanopositioning for high-speed spm. *J. Dyn. Syst. Meas. Contr.*, 131(6), 061101.

Croft, D., Shed, G., and Devasia, S. (2001). Creep, hysteresis, and vibration compensation for piezoactuators: atomic force microscopy application. *J. Dyn. Syst. Meas. Contr.*, 123(1), 35–43.

Galinaitis, W.S. (1999). *Two methods for modeling scalar hysteresis and their use in controlling actuators with hysteresis*. Ph.D. thesis, Virginia Tech.

Gozen, B.A. and Ozdoganlar, O.B. (2012). Design and evaluation of a mechanical nanomanufacturing system for nanomilling. *Precis. Eng.*, 36(1), 19 – 30.

Gu, G.Y., Zhu, L.M., Su, C.Y., Ding, H., and Fatikow, S. (2016). Modeling and control of piezo-actuated nanopositioning stages: A survey. *IEEE Trans. Automat. Sci. Eng.*, 13(1), 313–332.

Gu, G. and Zhu, L. (2011). Modeling of rate-dependent hysteresis in piezoelectric actuators using a family of ellipses. *Sens. Actuators, A*, 165(2), 303 – 309.

Jung, H. and Gweon, D.G. (2000). Creep characteristics of piezoelectric actuators. *Rev. Sci. Instrum.*, 71(4), 1896–1900.

Kuhnen, K. (2005). Modelling, identification, and compensation of complex hysteretic and log (t)-type creep nonlinearities. *Control and intelligent systems*, 33(2), 134–147.

Kuhnen, K. (2008). *Kompensation komplexer gedächtnisbehafteter Nichtlinearitäten in Systemen mit aktiven Materialien: Grundlagen - erweiterte Methoden - Anwendungen*. Berichte aus der Steuerungs- und Regelungstechnik. Shaker.

Mayergoyz, I.D. (2003). *Mathematical models of hysteresis and their applications*. Academic Press.

Natale, C., Velardi, F., and Visone, C. (2001). Identification and compensation of preisach hysteresis models for magnetostrictive actuators. *Physica B*, 306(1-4), 161 – 165.

Nelson, B.J., Dong, L., and Arai, F. (2008). *Micro/Nanorobots*, chapter Micro/Nanorobots, 411 – 450. Springer Science & Business Media.

Pesotski, D. (2011). *Echtzeit-Kompensation von komplexen hysterese-und kriechbehafteten Nichtlinearitäten am Beispiel von Festkörperaktoren*. Logos Verlag Berlin GmbH.

Rosenbaum, S., Ruderman, M., Strohla, T., and Bertram, T. (2010). Use of jiles–atherton and preisach hysteresis models for inverse feed-forward control. 46(12), 3984–3989.

Song, G., Zhao, J., Zhou, X., and Abreu-Garcia, J.A.D. (2005). Tracking control of a piezoceramic actuator with hysteresis compensation using inverse preisach model. *IEEE/ASME Trans. Mechatron.*, 10(2), 198–209.

Tan, X. and Baras, J.S. (2004). Recursive identification of hysteresis in smart materials. In *Proc. of the American Control Conference*, volume 4, 3857–3862.

Tian, Y., Zhang, D., and Shirinzadeh, B. (2011). Dynamic modelling of a flexure-based mechanism for ultra-precision grinding operation. *Precis. Eng.*, 35(4), 554 – 565.

Visintin, A. (2013). *Differential models of hysteresis*, volume 111. Springer Science & Business Media.

Webb, G.V., Lagoudas, D.C., and Kurdila, A.J. (1998). Hysteresis modeling of sma actuators for control applications. *Journal of Intelligent Material Systems and Structures*, 9(6), 432–448.

Xu, Q. and Tan, K.K. (2015). *Advanced control of piezoelectric micro-/nano-positioning systems*. Springer.

Zhao, X. and Tan, Y. (2008). Modeling hysteresis and its inverse model using neural networks based on expanded input space method. *IEEE Trans. Contr. Syst. Technol.*, 16(3), 484–490.